Spectral domain optical coherence tomography with sub-micrometer sensitivity for measurement of central corneal thickness

Lida Zhu (朱礼达)[1], Yi Wang (王 毅)[2,*], Yi Yuan (袁 毅)[1], Hongxian Zhou (周红仙)[3], Yuqian Zhao (赵玉倩)[2], and Zhenhe Ma (马振鹤)[2]

[1]*School of Electrical Engineering, Yanshan University, Qinhuangdao 066004, China*
[2]*School of Control Engineering, Northeastern University at Qinhuangdao, Qinhuangdao 066004, China*
[3]*Experiment Education Center, Northeastern University at Qinhuangdao, Qinhuangdao 066004, China*
**Corresponding author: wangyi@neuq.edu.cn*

Received October 31, 2018; accepted January 10, 2019; posted online April 1, 2019

We demonstrated a method for measurement of central corneal thickness (CCT) with a sub-micrometer sensitivity using a spectral domain optical coherence tomography system without needing a super broad bandwidth light source. By combining the frequency and phase components of Fourier transform, the method is capable of measurement of a large dynamic range with a high sensitivity. Absolute phases are retrieved by comparing the correlations between the detected and simulated interference fringes. The phase unwrapping ability of the present method was quantitatively tested by measuring the displacement of a piezo linear stage. The human CCTs of six volunteers were measured to verify its clinical application. It provides a potential tool for clinical diagnosis and research applications in ophthalmology.

OCIS codes: 170.4500, 170.4460, 120.3180.
doi: 10.3788/COL201917.041701.

Evaluation of central corneal thickness (CCT) plays an important role in clinical diagnosis and research applications in ophthalmology. CCT has been recognized as a credible indicator of the glaucoma damage and progression of ocular hypertension in primary open-angle glaucoma (POAG) patients[1–3]. It is also reported to have a positive correlation with intraocular pressure (IOP), which is a key risk factor for the development of glaucoma[4,5]. CCT is usually about 500–600 μm in normal subjects, and it statistically decreases by about 2–10 μm per decade[2]. Precise measurement of CCT has become more and more important with the booming development of refractive eye surgery. Ultrasonic and optical methods are the commonly used methods for CCT measurement. The ultrasonic method (ultrasonic pachymetry, USP) uses high-frequency sound waves (20 to 50 MHz) to detect the time lapse of reflected sound waves from the anterior and posterior corneal surfaces. USP has been regarded as the gold standard for many years due to its reliability and utility. However, USP has several disadvantages, including direct contact of the probe with the cornea with topical anesthesia, risk of infection and damage of the corneal epithelium, and examiner dependence.

In recent years, optical coherence tomography (OCT) [also referred as low-coherence interferometry (LCI), white light interferometry (WLI), or partial coherence reflectometry (PCR)] has been developed for CCT measurement. OCT is a noninvasive modality capable of investigating micro-structures[6–11]. Compared with USP, OCT has obvious advantages, such as high resolution, non-contact, and easy operation[12,13]. In laser refractive surgery, according to Munnerlyn's formula, the ablation depth is approximately 3 μm per diopter for an optical zone of 3 mm diameter to correct myopia[6]. Each laser pulse results in an ablation depth of about 0.2–0.3 μm in the corneal stroma[7,8]. The current OCT cannot measure the intraoperative or postoperative CCT changes with such sensitivity. The theoretical axial resolution of OCT is equal to $0.44\lambda^2/n\Delta\lambda$, where n is the refractive index, λ and $\Delta\lambda$ denote the center wavelength and the spectral bandwidth of the light source, respectively. For example, the light source centered at 1310 or 840 nm with a spectral bandwidth of 60 nm results in a theoretical axial resolution of 9.2 or 3.8 μm, respectively. Recently, several OCT systems with an ultra-high axial resolution up to ~1 μm have been reported[14–17]. Among all these techniques, ultra-high resolution is achieved by using a super broad bandwidth light source. However, such a light source is expensive, which prevents its prevalence. In traditional Fourier domain OCT (FD-OCT), depth information is demodulated from the frequency component by fast Fourier transform (FFT) of detected interference fringes, and such a demodulation method results in the limited axial sensitivity of FD-OCT. By analyzing the phase component of FFT, FD-OCT is able to achieve a super-high axial sensitivity up to the nanometer scale[18,19]. However, due to phase wrapping, phase imaging suffers from a limited dynamic range, which is restricted in $(-\pi, \pi]$, corresponding to an optical length difference (OLD) of half a wavelength. Phase wrapping issue occurs when the detected phase falls outside the range of $(-\pi, \pi]$ since the phase is periodic in nature. Many digital phase unwrapping algorithms have

been reported to address this problem[20,21]. However, these algorithms are valid only when the phase difference between neighboring pixels is less than π. This condition might be violated if the phase is discontinuous or noisy. So far, several techniques based on spectral domain OCT (SD-OCT) have been reported, attempting to extend the dynamic range of phase imaging. Hendargo *et al.* reported a synthetic wavelength-based method to extend the depth range without phase wrapping[22]. However, phase wrapping still occurs when OLDs exceed half a synthetic wavelength. Zhang *et al.* retrieved absolute phases by a least-square algorithm[23]. In both the methods, in order to eliminate the amplified phase noise, the retrieved unwrapped phase map is adopted as a reference to correct the wrapped phase obtained by FFT. But this correction may cause 2π errors due to the amplified noises of the reference phases[22,23]. Especially when the reference phase is close to an odd integer multiple of π, a low noise may lead to a phase error of 2π.

In this Letter, we demonstrate a method for CCT measurement with sub-micrometer sensitivity using an SD-OCT system without needing a super broad bandwidth light source, which is achieved by combining the frequency and phase components of FFT. First, an approximated OLD and a wrapped phase are calculated by FFT of detected interference fringes. Then, phase unwrapping is performed to retrieve the absolute phase by comparing the correlations between the detected and simulated interference fringes. Compared with the reported phase unwrapping methods using reference phases, the influence of amplified noises is eliminated. The method is capable of measurement of a large dynamic range with a high sensitivity.

The experimental setup, demonstrated in Fig. 1, mainly consists of an optical fiber-based Michelson interferometer and a homemade spectrometer. A superluminescent diode, centered at 1310 nm with a full width at half-maximum bandwidth of 68 nm, was used as the light source. The galvo scanner module allowed the sample light to image the area of interest. The sample light was focused onto the cornea by a lens with a focal length of 50 mm. The interference fringe formed by the light back-reflected from the reference and probing arms was captured by the homemade spectrometer. The spectrometer mainly consisted of a grating and a line scan CCD. The grating was 1145 lp/mm, and the line scan CCD (GL2048R, Sensors Unlimited) had 2048 pixels. The position of the eye under detection was adjusted with the assistance of an area camera, which provided real-time images of the eye. The incident power of the probing beam onto the cornea was 1.03 mW, which is much less than the standard permitted by the American National Standards for Safe Use of Lasers[24]. The system worked in two modes. When performing cross-section imaging, mirror M was used as the reference mirror to obtain the cross-section image of the cornea. The exposure time of the line scan CCD was set to be 80 μs, and 800 A lines were obtained to reconstruct the cross-section image. The total acquisition time was ~0.5 s. In CCT measurement mode, we used a common-path configuration to reduce the influence of ambient vibrations. The light back-reflected from mirror M was blocked out, and the interference fringe related to the light back-reflected from the anterior and posterior surfaces of the cornea was detected. The acquisition rate of the A line was 10 kHz, and 100 A lines were captured for calculating CCTs.

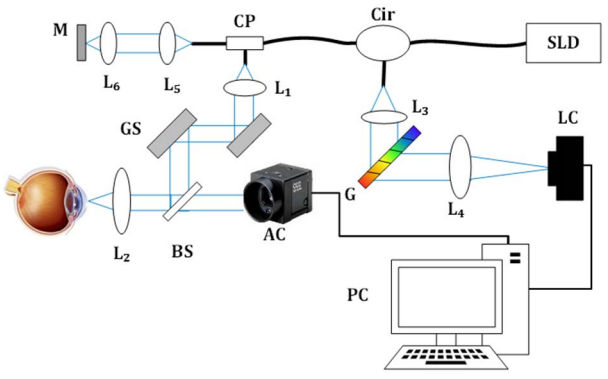

Fig. 1. Schematic of SD-OCT system. SLD, superluminescent diode; Cir, circulator; CP, coupler; GS, galvo scanner; BS, beam splitter; AC, area scan CCD; LC, line scan CCD; L_{1-6}, lens; M, mirror; G, grating.

In SD-OCT, the acquired interference fringe from a single sample reflector can be described as

$$I(k) = S(k)\{I_r + I_s + 2\sqrt{I_r I_s}\cos[k(m\Delta d + \sigma)]\}, \quad (1)$$

where k is the wavenumber, $S(k)$ is the power function of the light source, I_r and I_s denote the light intensities reflected from the reference surface and the sample, respectively. The absolute OLD between the reference and sample beams is equal to $(m\Delta d + \sigma)$, where m is an integer number, Δd denotes the resolution of FFT, $\Delta d = 2\pi/\Delta k$, Δk is the spectral width in the wavenumber of the spectrometer, and σ denotes the sub-resolution deviation. By applying FFT to the detected interference fringe, only the term $m\Delta d$ can be extracted due to the limited resolution of FFT and phase wrapping, which is an approximation to the total OLD $(m\Delta d + \sigma)$. The sensitivity of such demodulation is equal to Δd, which is about several microns. The remaining σ results in a phase shift of $\theta = k_c\sigma$, where k_c denotes the center wavenumber of the fringe. Let $\theta = \theta_0 + 2n_0\pi$, where θ_0 is restricted in $(-\pi, \pi]$ (i.e., the principle value or wrapped phase), and n_0 denotes an unknown integer number. Due to phase 2π ambiguity, only the principle value θ_0 can be obtained from the phase component of FFT. So phase unwrapping is required to precisely retrieve the total OLD as

$$\mathrm{OLD} = m\Delta d + \frac{\theta_0 + 2n_0\pi}{k_c}. \quad (2)$$

Compared with the term $m\Delta d$ obtained by direct FFT of the interference fringe, the total OLD can achieve

sub-nanometer sensitivity[23]. Here, we determine the unknown integer number n_0 by calculating the correlations between the detected and simulated spectral fringes. First, by FFT of the detected interference fringe, one can obtain the term $m\Delta d$ in Eq. (2) and the wrapped phase θ_0 from the frequency and phase components, respectively. Then, the simulated spectral fringe $I'(m\Delta d, \theta_0, n)$ can be generated as

$$I'(m\Delta d, \theta_0, n) = \cos\left[k'\left(m\Delta d + \frac{\theta_0 + 2n\pi}{k'_c}\right)\right], \quad n = 0, \pm 1, \pm 2, ..., \pm N, \tag{3}$$

where the systematic parameters k' (wavenumber axis), k'_c (center wavenumber), and Δd (resolution) can be precalibrated; n is an integer number representing the 2π order of phase wrapping; N is the searching range; and $N = \text{round}(\Delta d/2k'_c)$, where round() denotes the round operation. The OLD increment of the simulated fringes is $2\pi/k'_c$, corresponding to a phase shift of 2π. The detected fringe is compared with each simulated fringe in the SD. When the correlation between the detected and simulated fringe reaches the maximum, the unknown integer number n_0 is obtained to be the integer number that is adopted to generate the simulated fringe. The process steps are shown in Fig. 2, where Fig. 2(a) shows a representative detected fringe related to the light back-reflected from the anterior and posterior surfaces of the cornea. First, the DC component and high-frequency noises of the detected fringe are rejected by using a digital finite impulse response (FIR) band-pass filter, whose passband center frequency is close to $m\Delta d$, and the filtered fringe is normalized by the premeasured power function of the light source, as shown in Fig. 2(b). Second, the term $m\Delta d$ and the wrapped phase θ_0 in Eq. (2) related to the reshaped fringe [Fig. 2(b)] are calculated by using FFT, and a series of simulated fringes is generated according to Eq. (3). Then, the cross-correlation between the detected fringe and each simulated fringe is calculated to determine their correlations:

$$S(n) = \max|\text{corr}[I'(m\Delta d, \theta_0, n), I(m\Delta d, \theta_0)]|, \quad n = 0, \pm 1, \pm 2, ..., \pm N, \tag{4}$$

where $I(m\Delta d, \theta_0)$ is the reshaped detected fringe; max() and corr() denote the maximum-value and cross-correlation operations. When $S(n'_0)$ reaches the maximum, the unknown integer number n_0 involved in the detected fringe is obtained to be n'_0. The calculated $S(n)$ is plotted in Fig. 2(c), from which the unknown integer number n_0 is determined to be 12. Therefore, the true phase can be retrieved as $\theta = \theta_0 + 24\pi$, and consequently, the absolute OLD $= m\Delta d + (\theta_0 + 24\pi)/k'_c$. To clearly demonstrate the different correlations between the detected and simulated fringes, Fig. 2(d) displays the detected fringe and representative simulated fringes, where the dotted line is the detected fringe, and the blue line and the red line denote the simulated fringes with $n = 11$ and 12, respectively. It shows that the detected fringe is more correlated to the simulated fringe with $n = 12$, which is in agreement with the results shown in Fig. 2(c).

First, we quantitatively tested the phase unwrapping ability of the proposed method by measuring the displacement of a piezo linear stage. The linear stage was set in step-vibration mode with an amplitude of 3 μm. The results measured by the proposed method are displayed as the blue line in Fig. 3(a). The average step height is 2964.7 nm, and the relative error is 1.17%. For comparison, the red line depicts the wrapped result calculated by FFT, and the unwrapped result using the digital unwrapping function of MATLAB is shown as the black line. The results indicate that the step displacement can be correctly measured with high accuracy by the proposed method, and the traditional digital unwrapping method is invalid because the phase discontinuity related to the step edge is larger than π. In addition, we continuously measured the thickness of a coverslip in common-path configuration in about 10 s to evaluate the sensitivity and stability of the system. Figure 3(b) shows the histogram of the measured OLD fluctuations, and the standard

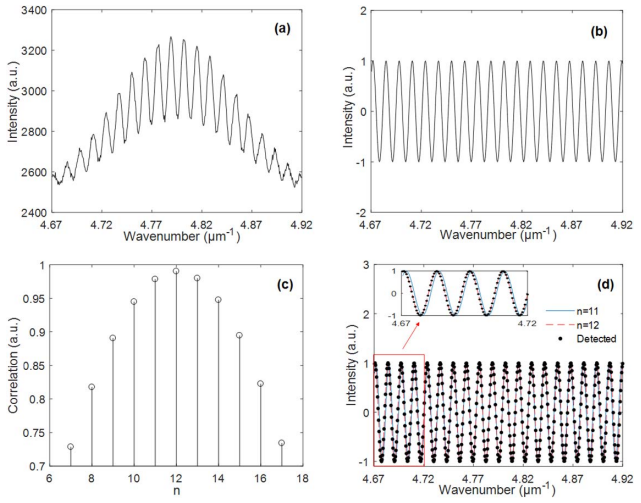

Fig. 2. Calculation of phase wrapping order. Acquired interference fringe (a) before and (b) after band-pass filtering and normalization. (c) Correlations between detected and simulated fringes. (d) Comparison of detected fringes with simulated fringes.

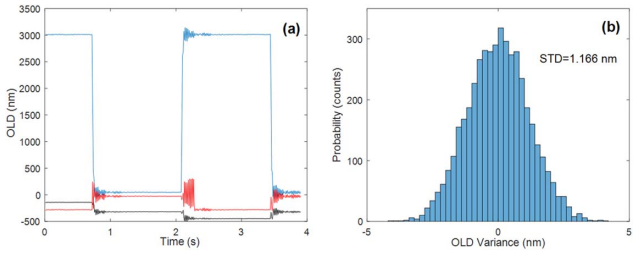

Fig. 3. (a) Red line depicts the wrapped result calculated by FFT; the result by applying digital unwrapping is shown as the black line, and the blue line shows the result by the proposed method. (b) Histogram of thickness variances of a coverslip.

deviation (STD) is 1.166 nm. It shows that the sensitivity of the system reaches the nanometer level.

To demonstrate the potential clinical application of the proposed method, the CCTs of six healthy volunteers aged about 25 years were measured. Figure 4(a) is a typical cross-section image of the cornea provided by the SD-OCT system. Figure 4(b) shows the A-scan profile of the central cornea at the meridian, and the CCT is 562.1 μm calculated by the traditional demodulation method of SD-OCT and 559.39 μm by the proposed method, using a corneal refractive index of 1.373. The sensitivity of the traditional demodulation method was measured to be $7.283 = 1.82\ \text{mm} \times 1000/250\ \mu\text{m}$ in tissue. 100 A lines of the left eye of each volunteer were sampled continuously to calculate the CCTs. Figure 5 is the boxplots of the experimental results. On each box, the central red line indicates the median, and the bottom and top edges of the box indicate the 25th and 75th percentiles, respectively. The lines above and below the box show the locations of the minimum and maximum. The average CCTs of the six subjects distribute from 507.70 to 582.43 μm, locating in the CCT range of normal human eyes. The data of subjects 2, 3, 5, and 6 reveal an excellent stability and reproducibility, and their maximum deviations from the corresponding averages are less than 0.1 μm. The data of subject 4 show a relatively large deviation (1.86 μm), which results from eye tremor. The boxplot of subject 1 has two outliers labeled with red '+', but still shows a small deviation (less than 0.2 μm). The average STD of the six data sets is 0.18 μm. The sensitivity of the system is changed from 1.166 nm for measurement of a coverslip to 0.18 μm for CCT measurement.

The above experimental results verified that the proposed method can be used for measuring the human

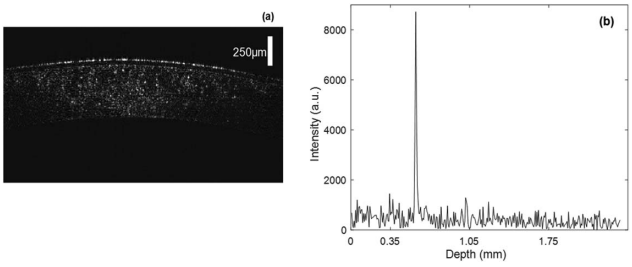

Fig. 4. (a) Cross-section image of cornea. (b) A-scan profile of central cornea at the meridian.

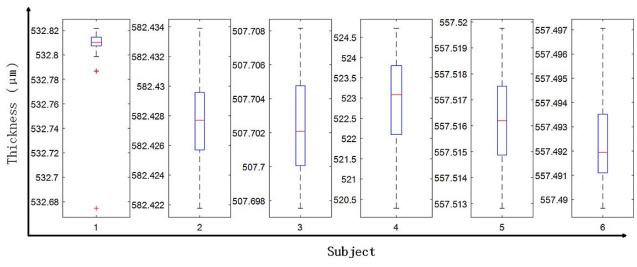

Fig. 5. Boxplots of the results of CCT measurement.

CCT with high resolution and high stability. This method can be applied on a traditional SD-OCT system without needing a super broad bandwidth light source. Compared with the reported ultra-high OCT systems, the proposed method achieves sub-micrometer sensitivity by combining the frequency and the phase components of FFT. The frequency component gives a relatively large dynamic range but low resolution. The phase component can achieve a high resolution up to nanometer or sub-nanometer, but suffers from a limited detective range (half a wavelength) due to phase wrapping. In contrast to the reported methods that require an unwrapped reference phase to retrieve the absolute phase, we calculate the absolute phase by comparing the correlations between the detected and simulated fringes. So, the influence of the amplified noises of the reference phase is eliminated.

We note that the present method is only suitable for measurement of the layers that can be distinguished by the traditional demodulation method of SD-OCT. It means that the present method is incapable of measurement of the thin layers with a thickness less than the resolution determined by traditional SD-OCT. The validity of the method is also dependent on the signal-to-noise ratio (SNR) of the detected fringe. Poor SNR may cause wrong correlations between the detected and simulated fringes, leading to an error to the integer number n_0, as shown in Eq. (2). A ± 1 error of n_0 leads to an OLD error of half a wavelength, i.e., ± 0.48 μm for CCT measurement.

In conclusion, we have demonstrated a method for CCT measurement with sub-micrometer sensitivity using an SD-OCT system without needing a super broad bandwidth light source. It is achieved by combining the frequency and phase components of FFT. We retrieve the absolute phase by comparing the correlations between the detected and simulated interference fringes. The phase unwrapping ability was quantitatively tested by measuring the displacement of a piezo linear stage. The human CCTs of six volunteers were measured to verify its clinical application. It provides a potential tool for clinical diagnosis and research applications in ophthalmology.

This research was supported in part by the National Natural Science Foundation of China (NSFC) (Nos. 61275214, 31170956, and 61771119), the Natural Science Foundation of Hebei Province, China (Nos. A2015501065 and H2015501133), and the Fundamental Research Funds for Central Universities (No. N172304034).

References

1. L. W. Herndon, J. S. Weizer, and S. S. Stinnett, Arch. Opthalmol.-Chic. **122**, 17 (2004).
2. C. C. Sng, M. Ang, and K. Barton, Curr. Opin. Opthalmol. **28**, 120 (2016).
3. J. D. Brandt, J. A. Beiser, M. A. Kass, and M. O. Gordon, Ophthalmology **108**, 1779 (2001).
4. M. C. Leske, A. Heijl, L. Hyman, B. Bengtsson, L. Dong, and Z. Yang, EMGT Group Ophthalmol. **114**, 1965 (2007).

5. W. A. Argus, Ophthalmology **102**, 1810 (1995).
6. C. R. Munnerlyn, S. J. Koons, and J. Marshall, J. Cataract. Refr. Surg. **14**, 46 (1988).
7. F. Kremer, M. Aronsky, B. Bowyer, and S. X. Stevens, Cornea **21**, 28 (2002).
8. R. R. Krueger and S. L. Trokel, Arch. Opthalmol.-Chic. **103**, 1741 (1985).
9. D. Huang, E. A. Swanson, C. P. Lin, J. S. Schuman, W. G. Stinson, W. Chang, M. R. Hee, T. Flotte, K. Gregory, and C. A. Puliafito, Science **254**, 1178 (1991).
10. A. F. Fercher, J. Biomed. Opt. **1**, 157 (1996).
11. J. J. Kałuzny, M. Wojtkowski, and A. Kowalczyk, Opt. Appl. **32**, 581 (2003).
12. D. Roshan, S. Hrebesh, N. Kai, M. M. Paul, H. Josh, W. Carol, and J. L. Martin, Chin. Opt. Lett. **15**, 090007 (2017).
13. J. Woo and W. Ruikang, Chin. Opt. Lett. **15**, 090005 (2017).
14. K. Bizheva, B. Tan, B. MacLelan, O. Kralj, M. Hajialamdari, D. Hileeto, and L. Sorbara, Biomed. Opt. Express **8**, 800 (2017).
15. R. Yadav, K.-S. Lee, J. P. Rolland, J. M. Zavislan, J. V. Aquavella, and G. Yoon, Biomed. Opt. Express **2**, 3037 (2011).
16. L. Liu, J. A. Gardecki, S. K. Nadkarni, J. D. Toussaint, Y. Yagi, B. E. Bouma, and G. J. Tearney, Nat. Med. **17**, 1010 (2011).
17. R. M. Werkmeister, A. Alex, S. Kaya, A. Unterhuber, B. Hofer, J. Riedl, M. Bronhagl, M. Vietauer, D. Schmidl, T. Schmoll, G. Garhöfer, W. Drexler, R. A. Leitgeb, M. Groeschl, and L. Schmetterer, Invest. Ophth. Vis. Sci. **54**, 5578 (2013).
18. Y. Yan, Z. Ding, Y. Shen, Z. Chen, C. Zhao, and Y. Ni, Opt. Express **21**, 25734 (2013).
19. C. Joo, T. Akkin, B. Cense, B. H. Park, and J. F. de Boer, Opt. Lett. **30**, 2131 (2005).
20. D. C. Ghiglia and L. A. Romero, J. Opt. Soc. Am. A **11**, 107 (1994).
21. S. Xia, Y. Huang, S. Peng, Y. Wu, and X. Tan, J. Biomed. Opt. **22**, 36014 (2017).
22. H. C. Hendargo, M. Zhao, N. Shepherd, and J. A. Izatt, Opt. Express **17**, 5039 (2009).
23. J. Zhang, B. Rao, L. Yu, and Z. Chen, Opt. Lett. **34**, 3442 (2009).
24. Z. Ansi, 136.1 American National Standard for Safe Use of Lasers, Laser Institute of America, Orlando, Florida (2000).